

Supplementary information

Template-free fabrication of magnetic mesoporous poly(ionic liquid)s: efficient interfacial catalysts for hydrogenation reaction and transesterification of soybean oil

Shengnan Li,^a Xiaotong Lu,^a Qi Liu,^a Limin Wang,^b Yujing Liu,^a Zhongqiu Liu,^a and Anguo Ying^{a,*}

^a *Department of Chemistry and Chemical Engineering, Qufu Normal University, Qufu, Shandong 273100, People's Republic of China*

^b *Department of History and Culture, Qufu Normal University, Qufu, Shandong 273100, People's Republic of China*

* Corresponding authors.

E-mail addresses: yinganguo@163.com (A. Ying).

List of the contents

1. Characterization.....	S1
2. Synthesis of terminal alkene modified Fe ₃ O ₄ @SiO ₂ nanoparticles.....	S1-S2
3. Preparation of functional 1,4-diazabicyclo[2.2.2]octane (FDABCO)....	S2
4. Table S1 to Table S3.....	S2-S3
5. Fig. S1 to Fig. S10.....	S4-S8
6. The GC-MS spectrum of the hydrogenation products.....	S9-S12
7. The GC-MS spectrum of transesterification.....	S12-S17
8. Reference.....	S17

1. Characterization.

All of the chemicals involved were commercially available without further purification and the water was deionized. Fourier transform infrared spectrometer (FTIR, NEXUS-470), Transmission electron microscopy (TEM, 80-200kVJEM-2100PLUS), X-ray diffractometer (XRD, PANalytical X-ray Diffractometer Model X pert3), hysteresis loop test (VSM, PPMS-9), Inductively coupled plasma (ICP), Thermogravimetric analyses (TGA), X-ray photoelectron spectroscopy (XPS), and water contact angle (WCA) were used to feature the morphology and structure of the samples. The surface area and pore size distribution were obtained via the N₂ adsorption-desorption isotherm and calculated by BET and BJH method respectively.

2. Synthesis of terminal alkene modified Fe₃O₄@SiO₂ nanoparticles.

Put the sodium dodecylbenzene sulphonate (SDBS, 26.25 g) and xylene (225 mL) into the beaker to obtain the dissolved SDBS solution completely by ultrasound treatment. Then put the FeCl₂ 4H₂O (2.235 g), Fe(NO₃)₃ 9H₂O (9.09 g), and H₂O (11.25 mL) into the beaker to obtain the dissolved mix salt solution completely by ultrasound treatment. Mixing the dissolved salt solution with the SDBS solution and stirring overnight. After that, heated the system to 90 °C and kept it for 1 h under the nitrogen atmosphere. Next added hydrazinium hydroxide solution (10.2 mL, 50 wt%) continued reacting 3 h. Then added tetraethyl orthosilicate (TEOS, 30 mL) for another

24 h with stirring vigorously when the system cooled down to 40 °C to prevent the complete evaporation of water. After the reaction was over, the products were washed successively with H₂O and methanol and separated by external magnetic force and put it in the oven at 80 °C for 5 h to get Fe₃O₄@SiO₂. Sodium dodecyl sulfate (SDS, 1 g) was dissolved in deionized H₂O (100 mL) to form the SDS solvent, then put it and Fe₃O₄@SiO₂ (1 g) to the round-bottom flask with ultrasound treatment for 20 min. Triethoxyvinylsilane (TEVS, 7 mL) was injected into the mixture solvent under the N₂ atmosphere and vigorous stirring, then the temperature was raised to 50 °C and kept stirring for 48 h. The final terminal alkene modified Fe₃O₄@SiO₂ were rigorously washed with H₂O and ethanol, then dried at 80 °C for 6 h.

3. Preparation of functional 1,4-diazabicyclo[2.2.2]octane (FDABCO).

1,4-Diazabicyclo[2.2.2]octane (25 mmol), 2-bromoethyl acrylate (25 mmol), and methanol (20 mL) were added to the flask, heated at 55 °C for 24 h under the N₂ atmosphere. After the reaction finished, the mixed coarse solvent was concentrated under reduced pressure to obtain the crude product. Then ethyl acetate was added to remove the unreacted compound, the product precipitated out by ultrasonic treatment and repeated the same operation three times.

Table S1. The surface area, pore size, and volume of Pd-p(3TEMPA-FDABCO-2DVB)@Fe₃O₄, p(3TEMPA-FDABCO-2DVB)@Fe₃O₄ in absence of terminal alkene modified Fe₃O₄@SiO₂ nanoparticles and various of p(xTEMPA-yFDABCO-zDVB)@Fe₃O₄.

Entry	Samples	S _{BET} ^a (m ² g ⁻¹)	D _{AV} ^b (nm)	V _{total} ^c (cm ³ g ⁻¹)
-------	---------	--	--------------------------------------	---

1	p(TEMPA-FDABCO-DVB) @Fe ₃ O ₄	272.49	4.27	0.5817
2	p(TEMPA-FDABCO-4DVB) @Fe ₃ O ₄	327.86	2.19	0.3597
3	p(2.5TEMPA-2.5FDABCO-DVB)@Fe ₃ O ₄	51.22	6.36	0.1629
4	p(3TEMPA-FDABCO-2DVB)@Fe ₃ O ₄	273.28	3.04	0.4154
5	p(TEMPA-3FDABCO-2DVB)@Fe ₃ O ₄	276.95	2.12	0.2933
6	Pd-p(3TEMPA-FDABCO-2DVB) ^d	3.4669	3.75	0.0819
7	Pd-p(3TEMPA-FDABCO-2DVB)@Fe ₃ O ₄	247.04	3.92	0.4838
8	p(FDABCO-2DVB)@Fe ₃ O ₄	76.24	2.43	0.2167

^a Brunauer-Emmett-Teller (BET) surface area was calculated over the relative pressure range of 0.05-0.20. ^b Average pore size. ^c Total pore volume. ^d Polymerization reaction in absence of terminal alkene modified Fe₃O₄@SiO₂ nanoparticles.

Table S2. The catalytic effect of different catalysts on styrene hydrogenation.

Entry	catalyst	Reaction time (min)	Reaction condition	Conv. (%)	Ref.
1	Pd-p(3TEMPA-FDABCO-2DVB) @Fe ₃ O ₄	10	25 °C, 101 kPa	>99	This work
2	[C ₄ AzoC ₂ DMEA]Br/Pd@SM	40	25 °C, 101 kPa	>99	Ref. ¹
3	Pd/MSS-C20	35	40 °C, 0.35 MPa	89	Ref. ²
4	Pd/SN-ON	90	40 °C, 0.35 MPa	>99	Ref. ³
5	Pd/PEG4000	90	25 °C, 101 kPa	60	Ref. ⁴

Table S3. Element distribution on terminal alkene modified of $\text{Fe}_3\text{O}_4@\text{SiO}_2$ and $\text{Pd-p}(x\text{TEMPA-}y\text{FDABCO-}z\text{DVB})@\text{Fe}_3\text{O}_4$.

Entry	Catalytic	Element distribution (%)			TEMPA loading (mmol g^{-1})	FDABCO loading (mmol g^{-1})	Pd (mmol g^{-1})
		C	N	O			
1	terminal alkene modified of $\text{Fe}_3\text{O}_4@\text{SiO}_2$	6.07	0.05	7.79	0	0	0
2	$\text{Pd-p}(3\text{TEMPA-FDABCO-O-2DVB})@\text{Fe}_3\text{O}_4$	58.74	6.13	12.91	0.53	0.19	0.2053
3	$\text{Pd-p}(\text{TEMPA-FDABCO-DVB})@\text{Fe}_3\text{O}_4$	52.47	5.62	12.63	0.61	0.17	0.1852
4	$\text{Pd-p}(2.5\text{TEMPA-2.5FDABCO-DVB})@\text{Fe}_3\text{O}_4$	51.23	4.67	12.89	1.02	0.12	0.1241
5	$\text{Pd-p}(3\text{TEMPA-FDABCO-O-2DVB})^a$	55.63	4.84	13.69	1.51	0.11	0.1048
6	$\text{Pd-p}(3\text{TEMPA-FDABCO-O-2DVB})@\text{Fe}_3\text{O}_4^b$	53.62	5.24	12.36	0.51	0.16	0.1733

^a $\text{Pd-p}(3\text{TEMPA-FDABCO-2DVB})$ without terminal alkene modified of $\text{Fe}_3\text{O}_4@\text{SiO}_2$.

^b $\text{Pd-p}(3\text{TEMPA}_3\text{-FDABCO-2DVB})@\text{Fe}_3\text{O}_4$ after 5 runs.

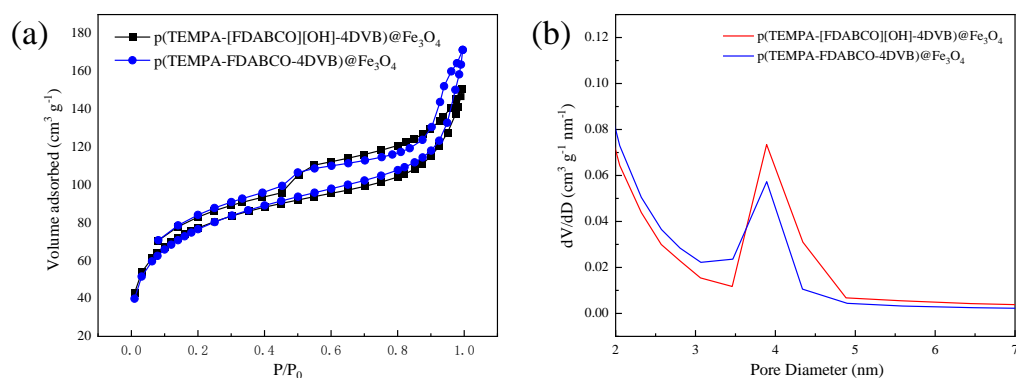


Fig. S1. N_2 adsorption/desorption isotherms (a) and the pore size distributions (b) of $\text{p}(\text{TEMPA-}[\text{FDABCO}][\text{OH}]\text{-4DVB})@\text{Fe}_3\text{O}_4$ and $\text{p}(\text{TEMPA-FDABCO-4DVB})@\text{Fe}_3\text{O}_4$.

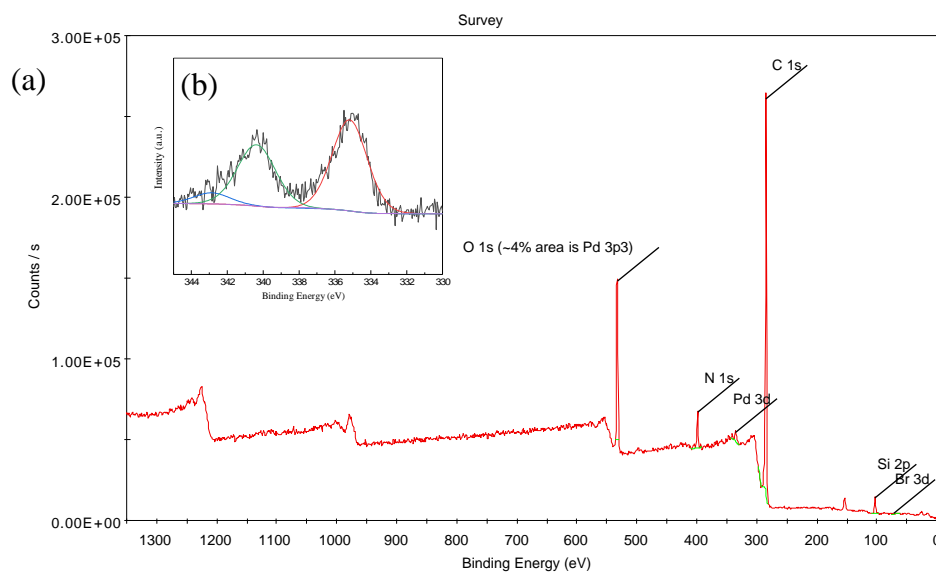


Fig. S2. (a) Full-range XPS spectrum; (b) Pd 3d spectrum of Pd-p(3TEMPA-FDABCO-2DVB)@Fe₃O₄.

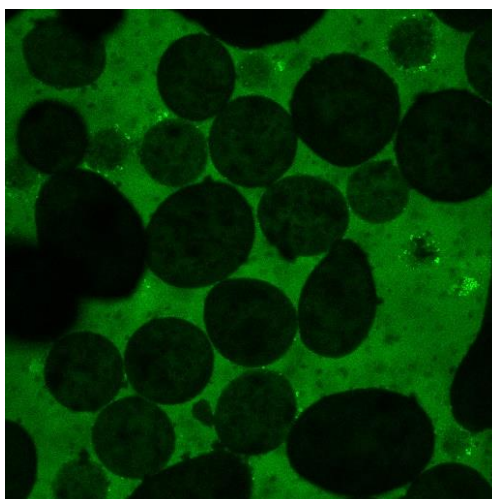


Fig. S3. Visual and confocal microscopy images of 20 mg Pd-p(3TEMPA-FDABCO-2DVB)@Fe₃O₄-stabilized Pickering emulsions with the volume ratio of water to *n*-octane (2:1).

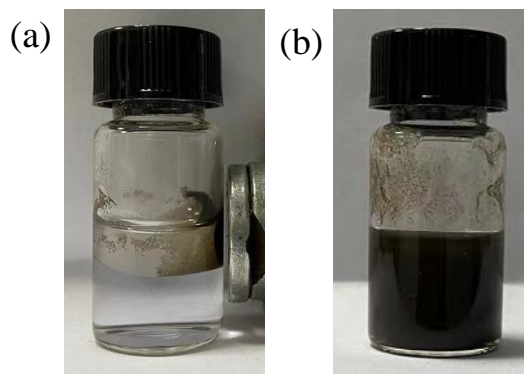


Fig. S4. The demulsification under magnetic and CO₂ (a); the Pickering emulsion with 20 mg Pd-p(3TEMPA-FDABCO-2DVB)@Fe₃O₄, *n*-octane/water (1 mL/2 mL) (b).

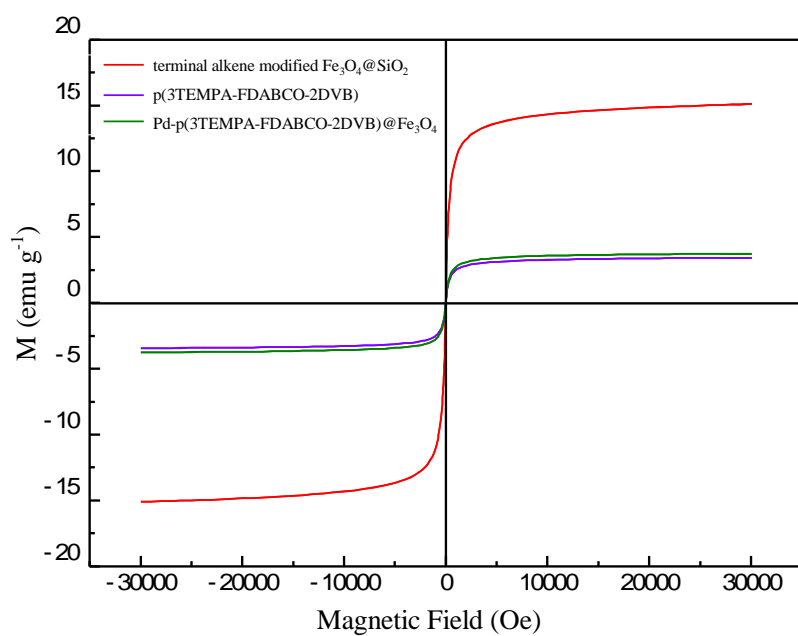


Fig. S5. Magnetization curves of terminal alkene modified Fe₃O₄@SiO₂, p(3TEMPA-FDABCO-2DVB)@Fe₃O₄, and Pd-p(3TEMPA-FDABCO-2DVB)@Fe₃O₄.

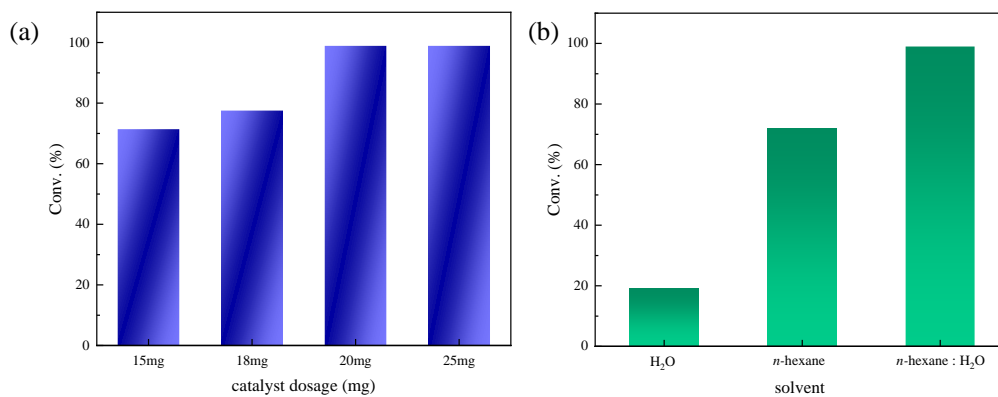


Fig. S6. Hydrogenation conversion rate of styrene with different catalyst dosage of Pd-p(3TEMPA-FDABCO-2DVB) $@\text{Fe}_3\text{O}_4$ (a) and different solvents (b). Reaction condition: 25 °C, 101 kPa, and mixture solvent ($V_{n\text{-hexane}} : V_{\text{H}_2\text{O}} = 1 : 2$).

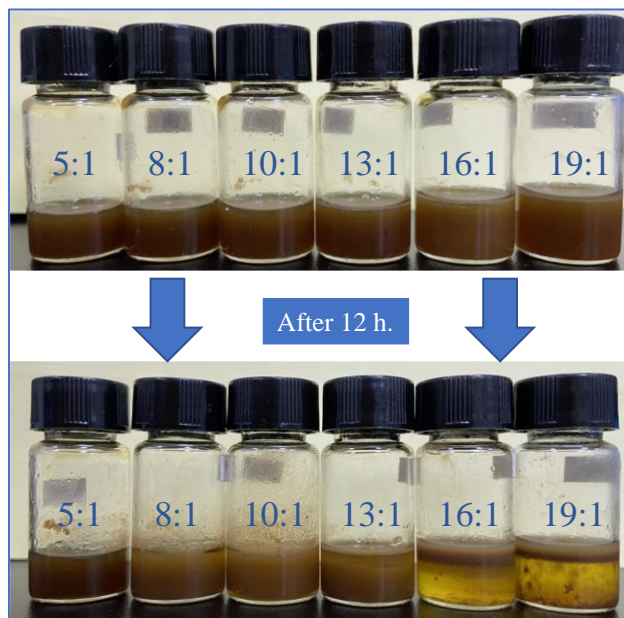


Fig. S7. The stability of the system with p(3TEMPA-[FDABCO][OH]-2DVB) $@\text{Fe}_3\text{O}_4$ under different ratios of ethanol/soybean oil.

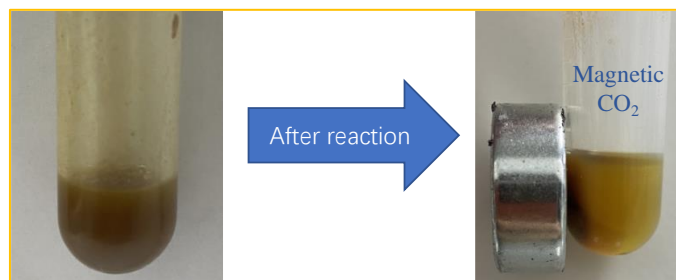


Fig. S8. Demulsification operation after transesterification reaction with dual-stimuli of the magnetic and CO_2 .

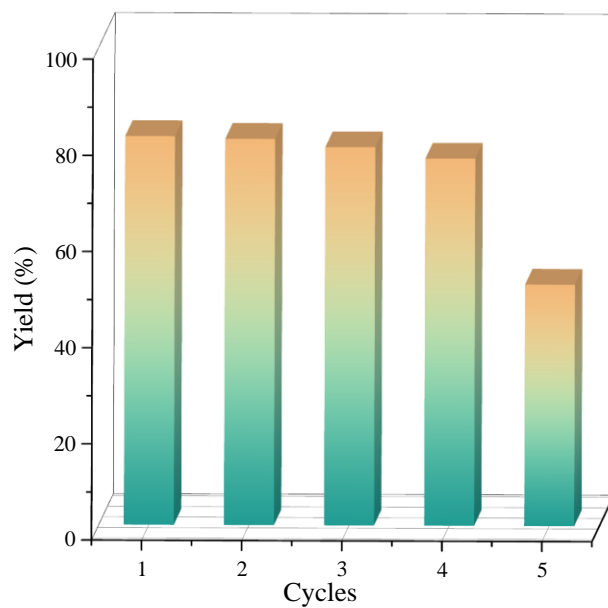


Fig. S9. Recycling test of transesterification catalytic by the p(3TEMPA-[FDABCO][OH]-2DVB)@Fe₃O₄.

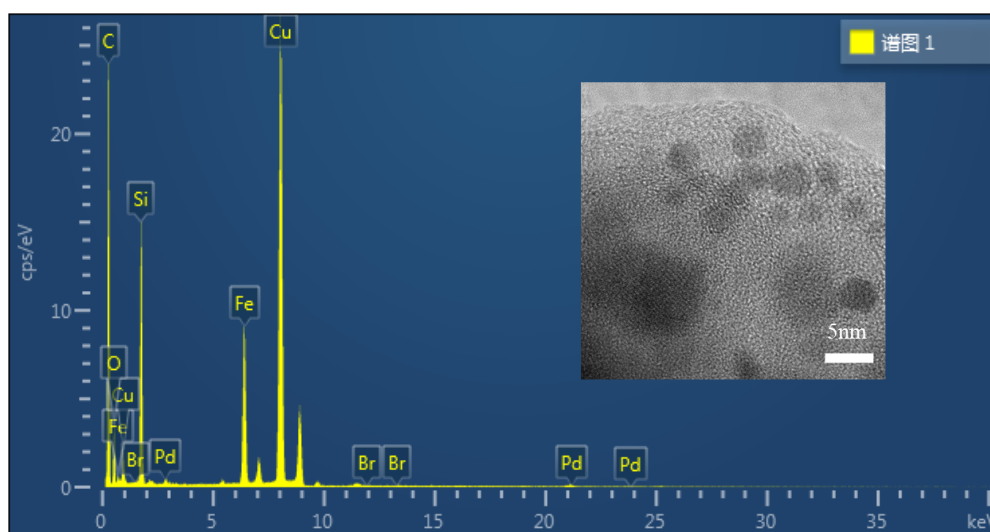


Fig. S10. The EDS spectrum of the Pd-p(3TEMPA-FDABCO-2DVB)@Fe₃O₄.

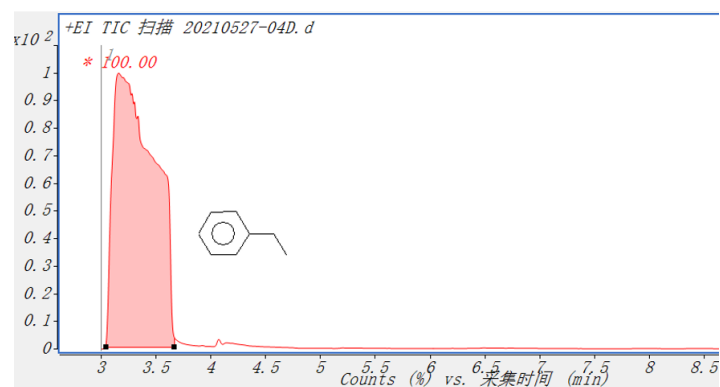


Fig. S11. The GC-MS spectrum of the hydrogenation (table 1 of main text, entry 1).

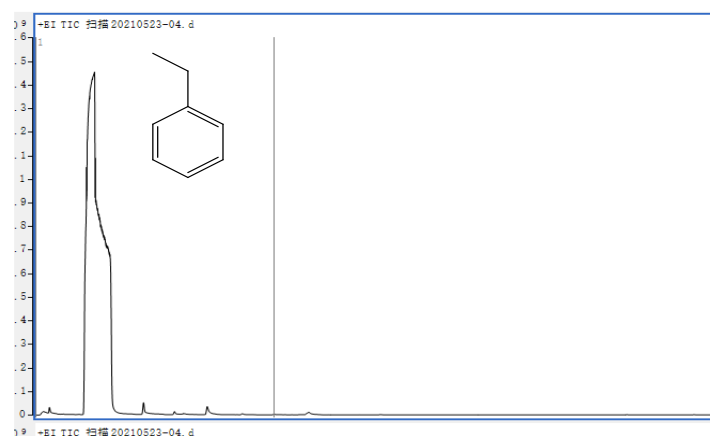


Fig. S12. The GC-MS spectrum of the hydrogenation (table 1 of main text, entry 2).

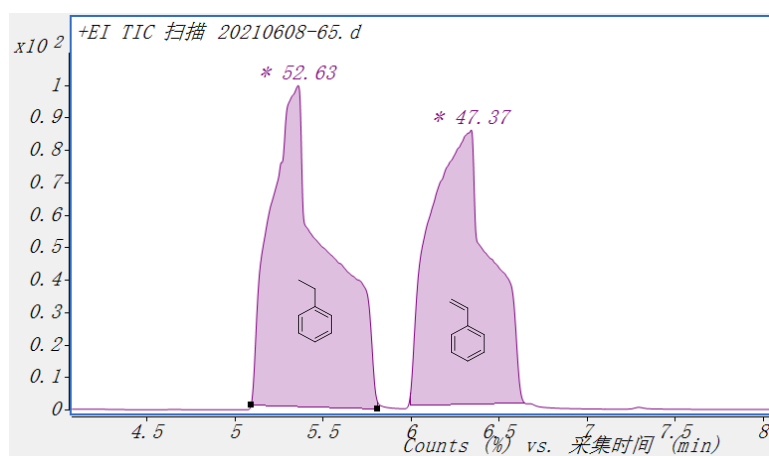


Fig. S13. The GC-MS spectrum of the hydrogenation (table 1 of main text, entry 3).

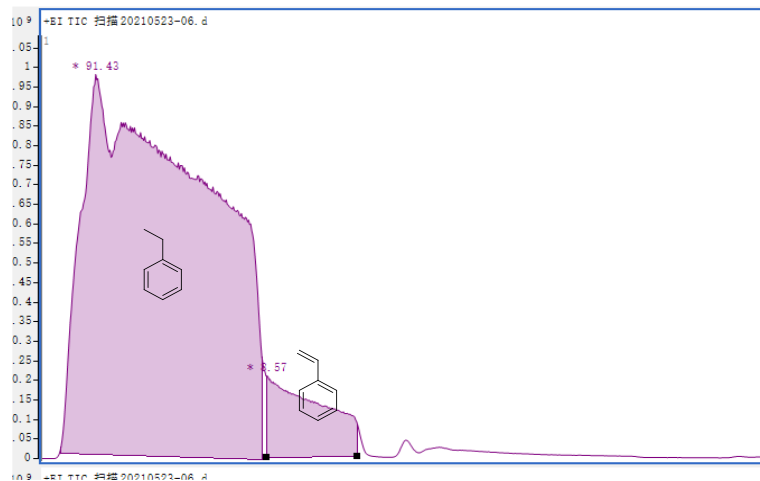


Fig. S14. The GC-MS spectrum of the hydrogenation (table 1 of main text, entry 4).

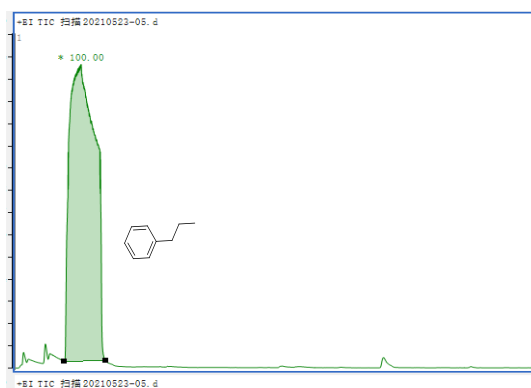


Fig. S15. The GC-MS spectrum of the hydrogenation (table 1 of main text, entry 5).

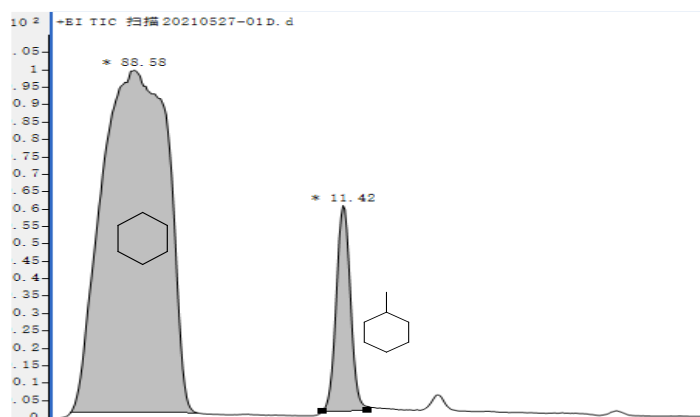


Fig. S16. The GC-MS spectrum of the hydrogenation (table 1 of main text, entry 6).

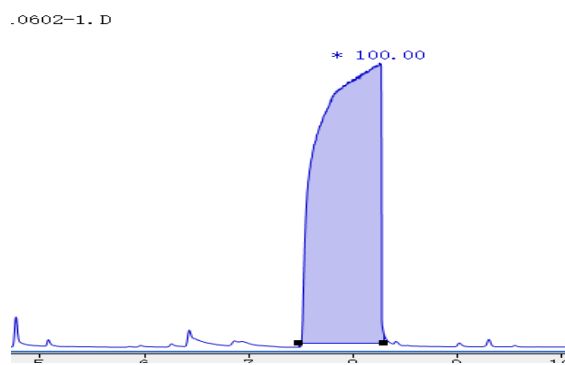


Fig. S17. The GC-MS spectrum of the hydrogenation (table 1 of main text, entry 7).

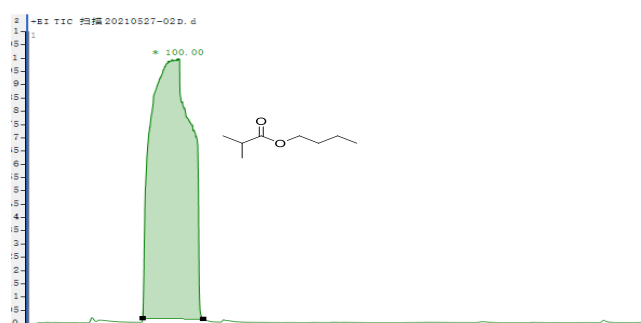


Fig. S18. The GC-MS spectrum of the hydrogenation (table 1 of main text, entry 8).

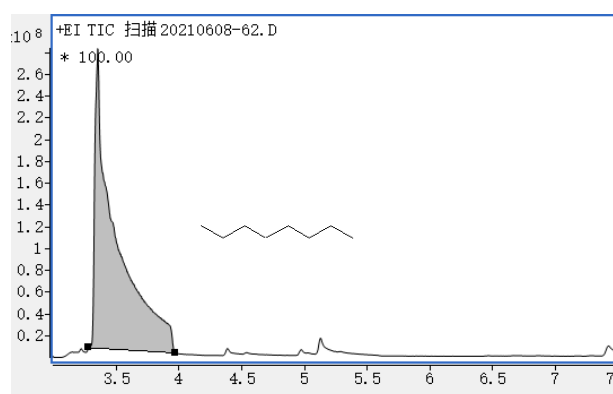


Fig. S19. The GC-MS spectrum of the hydrogenation (table 1 of main text, entry 9).

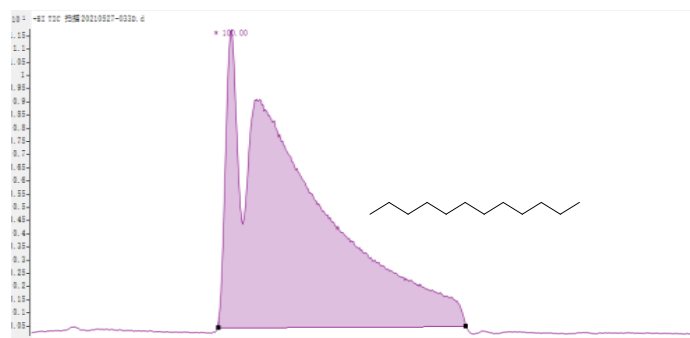


Fig. S20. The GC-MS spectrum of the hydrogenation (table 1 of main text, entry 10).

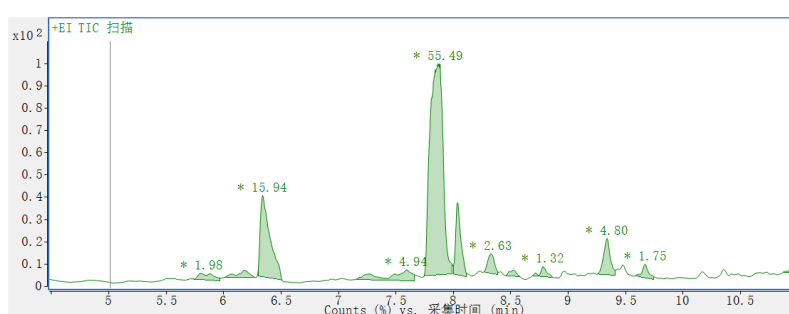


Fig. S21. The GC-MS spectrum of transesterification catalytic by p(3TEMPA-[FDABCO][OH]-2DVB)@Fe₃O₄.

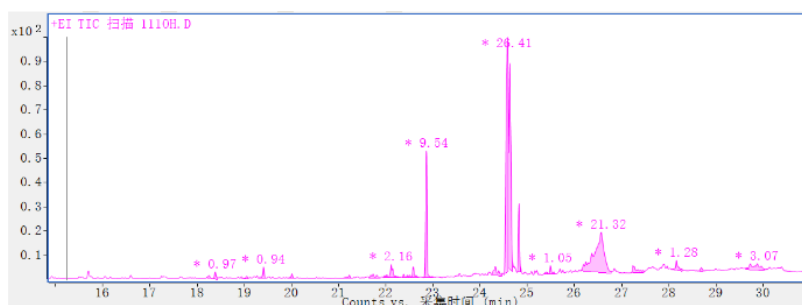


Fig. S22. The GC-MS spectrum of transesterification catalytic by p(TEMPA-[FDABCO][OH]-DVB)@Fe₃O₄.

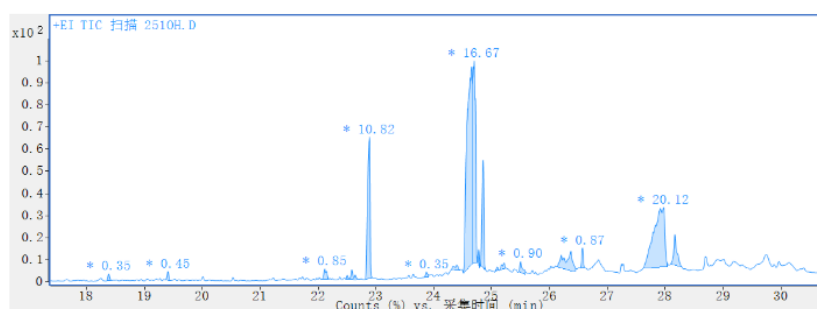


Fig. S23. The GC-MS spectrum of transesterification catalytic by p(2.5TEMPA-2.5[FDABCO][OH]-DVB)@Fe₃O₄.

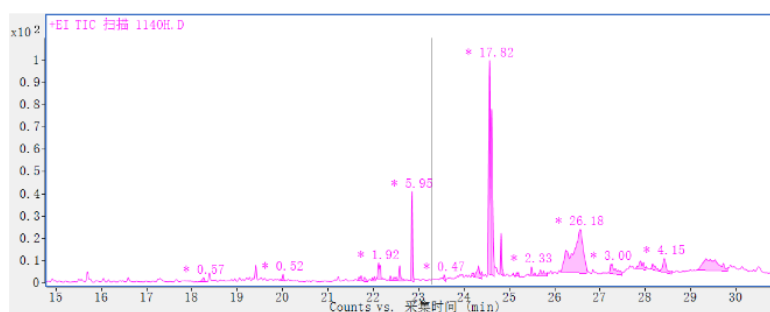


Fig. S24. The GC-MS spectrum of transesterification catalytic by p(TEMPA-[FDABCO][OH]-4DVB)@Fe₃O₄.

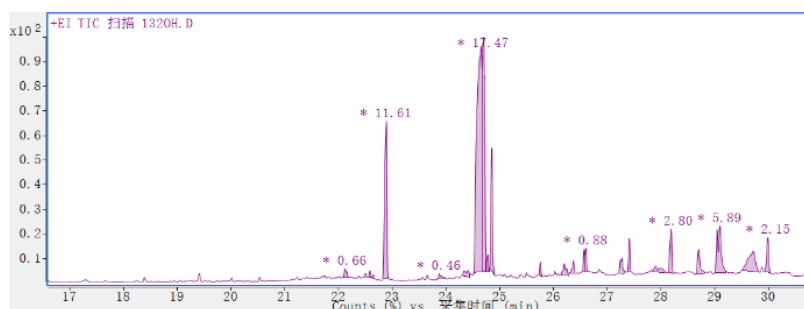


Fig. S25. The GC-MS spectrum of transesterification catalytic by p(TEMPA-3[FDABCO][OH]-2DVB)@Fe₃O₄.

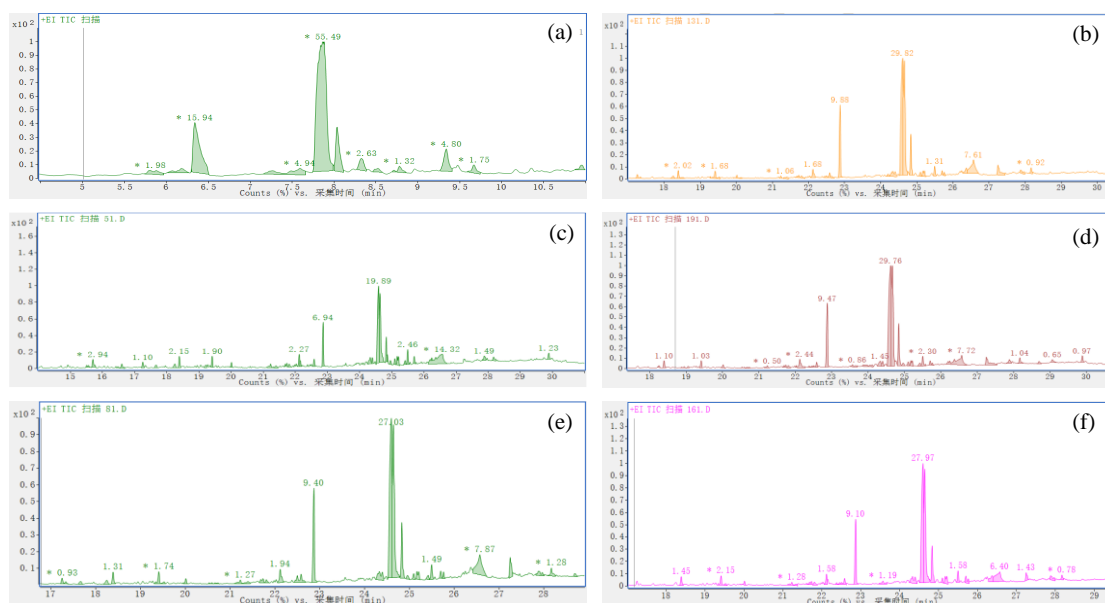


Fig. S26. The GC-MS spectrum of transesterification catalytic by p(3TEMPA-[FDABCO][OH]-2DVB)@Fe₃O₄ and different molar ratio of ethanol/soybean oil (a = 10:1; b = 13:1; c = 5:1; d = 19:1; e = 8:1; f = 16:1).

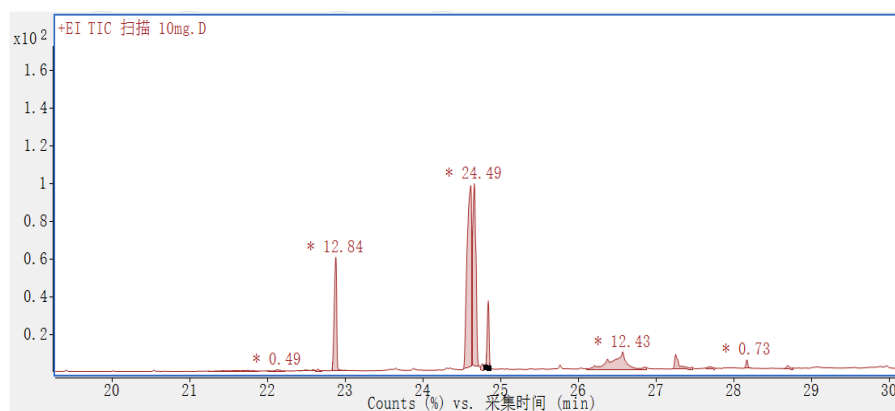


Fig. S27. The GC-MS spectrum of transesterification catalytic by p(3TEMPA-[FDABCO][OH]-2DVB)@Fe₃O₄ (10 mg).

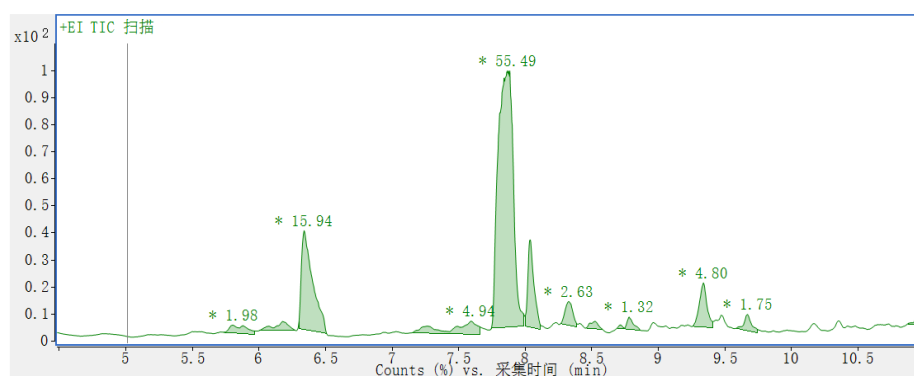


Fig. S28. The GC-MS spectrum of transesterification catalytic by p(3TEMPA-[FDABCO][OH]-2DVB)@Fe₃O₄ (20 mg).

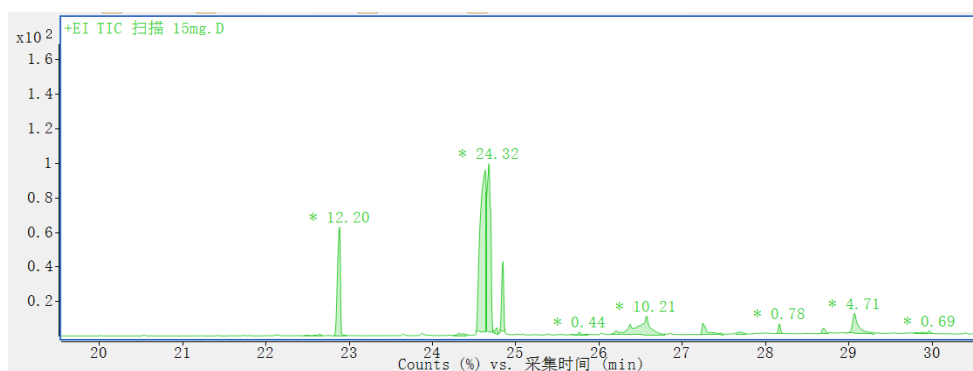


Fig. S29. The GC-MS spectrum of transesterification catalytic by p(3TEMPA-[FDABCO][OH]-2DVB)@Fe₃O₄ (15 mg).

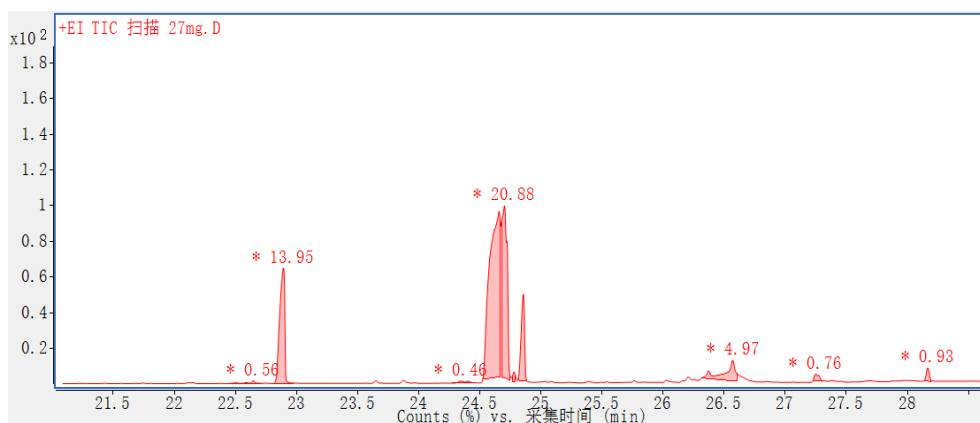


Fig. S30. The GC-MS spectrum of transesterification catalytic by p(3TEMPA-[FDABCO][OH]-2DVB)@Fe₃O₄ (27 mg).

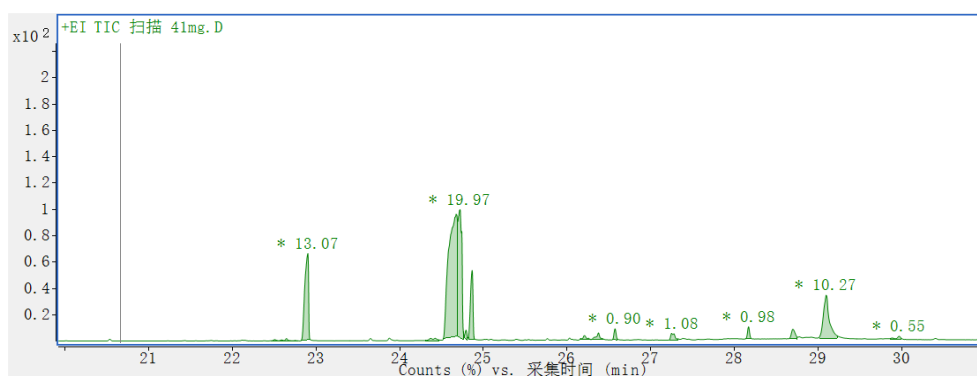


Fig. S31. The GC-MS spectrum of transesterification catalytic by p(3TEMPA-[FDABCO][OH]-2DVB)@Fe₃O₄ (41 mg).

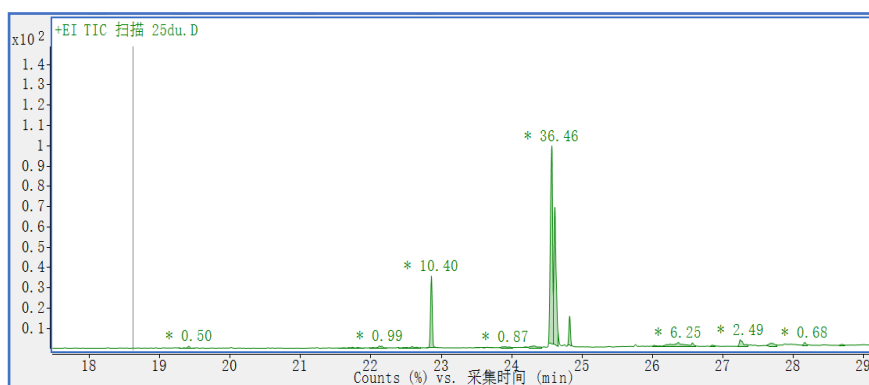


Fig. S32. The GC-MS spectrum of transesterification catalytic by p(3TEMPA-[FDABCO][OH]-2DVB)@Fe₃O₄ under 25 °C.

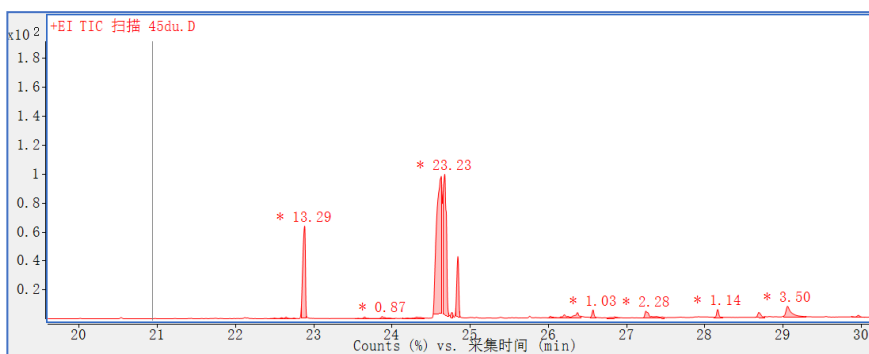


Fig. S33. The GC-MS spectrum of transesterification catalytic by p(3TEMPA-[FDABCO][OH]-2DVB)@Fe₃O₄ under 45 °C.

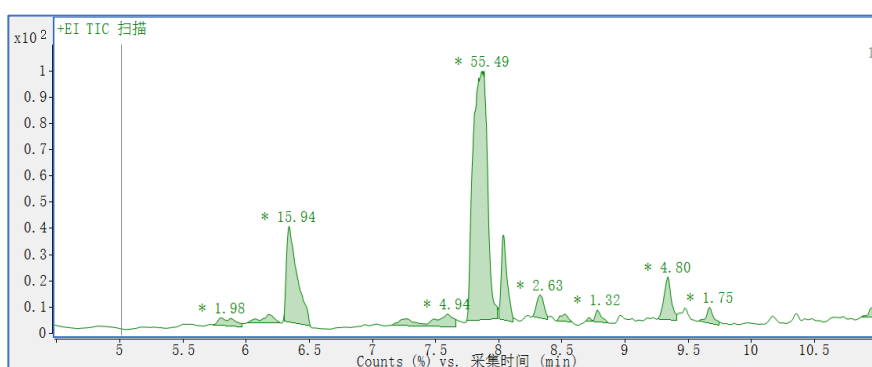


Fig. S34. The GC-MS spectrum of transesterification catalytic by p(3TEMPA-[FDABCO][OH]-2DVB)@Fe₃O₄ under 65 °C.

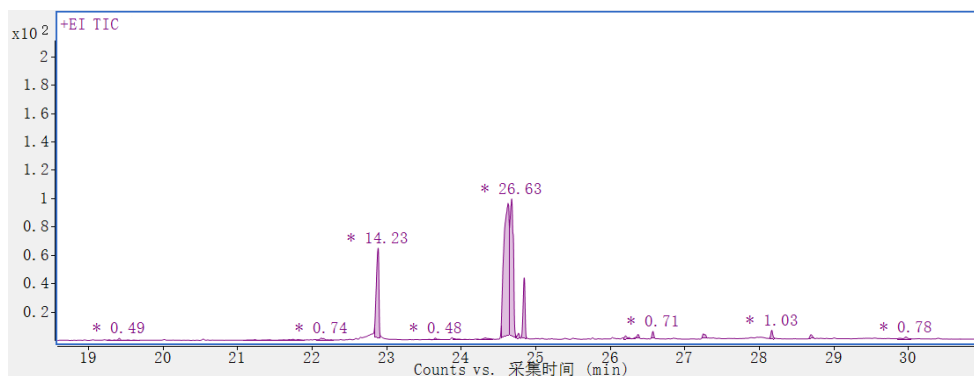


Fig. S35. The GC-MS spectrum of transesterification catalytic by p(3TEMPA-[FDABCO][OH]-2DVB)@Fe₃O₄ under 90 °C.

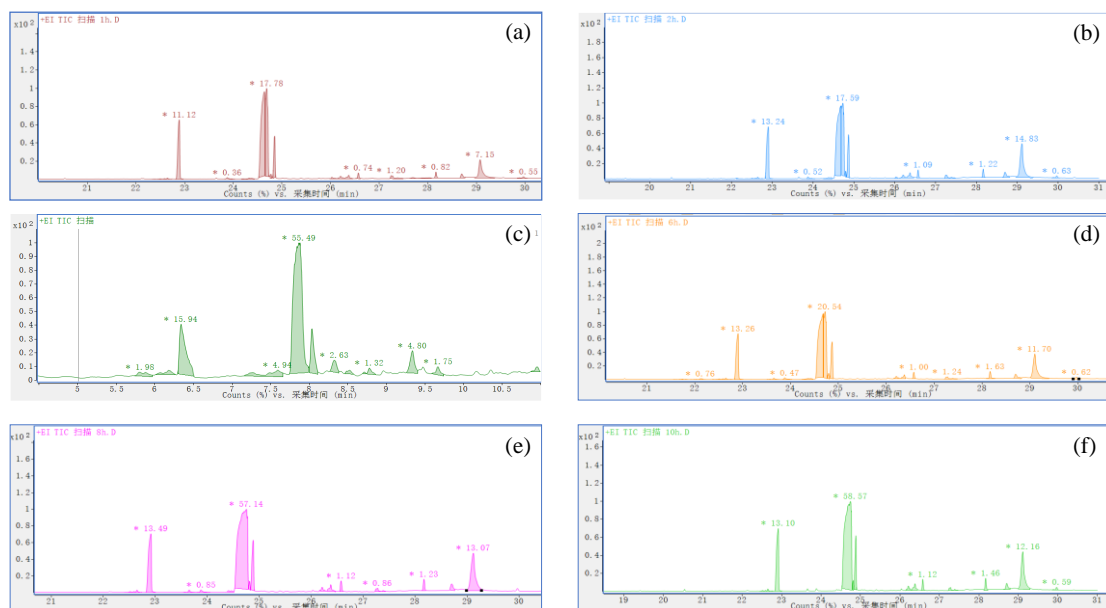


Fig. S36. The GC-MS spectrum of transesterification catalytic by $p(3\text{TEMPA}[\text{FDABCO}][\text{OH}]-2\text{DVB})@\text{Fe}_3\text{O}_4$ for different times (a = 1 h; b = 2 h; c = 4 h; d = 6 h; e = 8 h; f = 10 h).

Reference.

1. Z. Li, Y. Shi, A. Zhu, Y. Zhao, H. Wang, B. P. Binks and J. Wang, *Angew Chem Int Ed Engl*, 2021, **60**, 3928-3933.
2. L. Fu, S. Li, Z. Han, H. Liu and H. yang, *Chem Commun (Camb)*, 2014, **50**, 10045-10048.
3. J. Huang and H. Yang, *Chem Commun (Camb)*, 2015, **51**, 7333-7336.
4. F. Harraz, S. El-Hout, H. Killa and I. Ibrahim, *Journal of catalysis*, 2012, **286**, 184-192.